Jpn. J. Infect. Dis., 68, 89–97, 2015

Original Article

Establishment of a Rabbit Model of Spinal Tuberculosis Using *Mycobacterium tuberculosis* Strain H37Rv

Xiaochen Liu[1], Wenxiao Jia[2]*, Hong Wang[2], Yunling Wang[2], Jingxun Ma[2], Hao Wang[2], Xuan Zhou[2], and Guohua Li[3]

[1]*Department of Image, the First Affiliated Hospital of XinJiang Medical University, Xinjiang; and* [2]*Department of Image and* [3]*Department of Spine surgery, the Second Affiliated Hospital of XinJiang Medical University, Xinjiang, China*

SUMMARY: This study aimed to establish a spinal tuberculosis model by implanting *Mycobacterium tuberculosis* strain H37Rv into the lumbar vertebral body of New Zealand white rabbits. A hole was first drilled into the top of the 6th lumbar vertebra of each rabbit, which was then filled with a gelatin sponge to adsorb 0.2 ml of *M. tuberculosis* suspension (10^7 CFU /ml) for the infection group or normal saline for the control group. The holes were then closed with sutures. CT findings demonstrated that 5 and 10 rabbits developed spinal tuberculosis at 4 and 8 weeks, respectively, after this procedure. MRI examinations revealed that 7 and 15 rabbits had positive results at 4 and 8 weeks, respectively, after this procedure. HE staining of the vertebral body and paravertebral soft tissue biopsies of infected rabbits indicated inflammatory cell infiltration or necrosis in 15 rabbits. *M. tuberculosis* was cultured in 67% of the abscesses. The modeling success rate was 68.1%. By implanting an appropriate dosage of *M. tuberculosis* strain H37Rv into a local lumbar vertebral body of New Zealand white rabbits, we successfully established a spinal tuberculosis model, the pathological changes of which are similar to those of human spinal tuberculosis.

INTRODUCTION

Spinal tuberculosis (TB), also known as Pott's disease, is characterized by the destruction of the disc space and adjacent vertebral bodies, abscess formation, collapse of spinal elements, and subsequent severe and progressive kyphosis and risk of complete paraplegia (1). Spinal TB is a destructive form of tuberculosis that results from the hematogenous spread of *Mycobacterium tuberculosis* into the dense vasculature of cancellous bone of vertebral bodies from the primary infection site of the lung or genitourinary system (1). Spinal TB accounts for half of all cases of musculoskeletal tuberculosis (2), although it only accounts for 1%–5% of all TB cases (3). The clinical manifestations of spinal TB are extremely protean and patients normally present with a combination of primary manifestations such as weight loss, fever, fatigue, and malaise as well as focal back pain (2).

A diagnosis of spinal TB usually relies on nonspecific clinical presentations rather than conventional microbiological tests because tissue biopsies available to detect *M. tuberculosis* are difficult to obtain (4). Consequently, there are frequently delays in the diagnosis and treatment of spinal TB. Current treatments include anti-tuberculosis treatment, which needs to be determined empirically well before establishing an etiological diagnosis, and surgical intervention, which is recommended for managing severe cases (1). However, the limited usefulness of vaccines and the emergence of drug resistance has resulted in challenges for treating spinal TB (5).

Animal models are verified to be important and necessary for screening new drugs and new vaccines and for a better understanding of host-pathogen relationships. Various animals, including mice, guinea pigs, rabbits, and monkeys, have been used to establish TB infection models using pure cultures of *M. tuberculosis* (5). However, experimental animal models for spinal TB are relatively rare at present. Rabbit may be an ideal animal model for spinal TB when considering the feasibility of their use for larger basic surgical operations, such as debridement and bone grafting and their considerable susceptibility to *M. tuberculosis* (6). *M. tuberculosis* strain H37Rv, which was initially derived from a clinical isolate, H37, is a pathogenic, aerobic, chemoorganotrophic, rod-shaped, nonmotile bacterium that causes tuberculosis. It is a virulent strain that has been widely used in research on tuberculosis (7–9).

Thus, in the present study, we attempted to establish a rabbit model of spinal TB using *M. tuberculosis* strain H37Rv and assessed the efficacy of this model based on radiographical analyses, histopathological examinations, and bacteriological tests.

Received April 9, 2014. Accepted July 15, 2014. J-STAGE Advance Publication November 25, 2014.
DOI: 10.7883/yoken.JJID.2014.147

*Corresponding author: Mailing address: Department of Image, the Second Affiliated Hospital of XinJiang Medical University, NO.38 South Lake East Road, ShuiMoGou Area, Urumqi, Xinjiang 830063, China. Tel: +8609915105607, Fax: +8609915105607, E-mail: wenxiaojia5@hotmail.com

MATERIALS AND METHODS

Animals, materials, and *M. tuberculosis* strain: We purchased 40 New Zealand white rabbits (aged 3–4 weeks; body weights of 3.25 ± 0.25 kg) from Xinjiang

Centers for Disease Control. *M. tuberculosis* strain H37Rv (ATCC36801) was from the Shanghai Institute of Biological Products.

***Mycobacterial* suspensions:** Single cell suspensions were prepared by trituration. A total of 3–4 *M. tuberculosis* colonies on agar slant culture medium were transferred to a homogenizer with a bamboo stick. An appropriate amount of saline was added into the homogenizer and the bacteria were homogenized. Saline (10 ml) was added to wash the homogenizer and the suspension was diluted with saline to 5 mg/ml (10^8 CFU/ml). A bacterial suspension was collected and diluted with saline to prepare suspensions of 5×10^{-1} mg/ml (10^7 CFU/ml), 5×10^{-2} mg/ml (10^6 CFU/ml), 5×10^{-3} mg/ml (10^5 CFU/ml), 5×10^{-4} mg/ml (10^4 CFU/ml) and 5×10^{-5} mg/ml (10^3 CFU/ml).

Animal model: All animal experimental protocols were approved by the Ethics Committee of Xinjiang Medical University.

After numbering and weighing, the 40 rabbits were randomly divided into 2 groups: A. rabbits treated with *M. tuberculosis* (infection group; $n = 30$); and B. rabbits treated with sterile normal saline (control group; $n = 10$). All rabbits were examined preoperatively by X-ray to exclude any with vertebral anomalies.

The rabbits were given small amounts of water and fasted for 12 h preoperatively. After disinfecting once with a 2% iodine tincture and twice with 75% alcohol, an ear vein was slowly injected with 2% barbital sodium idodine (20 mg/kg) for anesthesia. Then, the intravenous infusion needle was fixed with medical tape and connected to a T-branch tube that was sealed with 2–3 ml of a heparin saline solution (5 U/ml). Next, the rabbit was placed on an operating table while lying on its left side and the right lower back was shaved (10 cm × 15 cm). The surgical site and surrounding skin were disinfected successively with 2% Lysol, 70% alcohol, 5% tincture of iodine, and 75% alcohol, and then covered with a sterile drape with the surgical site exposed.

A longitudinal incision 6 cm long was made down from the 6th lumbar spinous process. The subcutaneous fascia and muscle were separated carefully so as to avoid injury to vessels and nerves and the 6th lumbar vertebra was completely exposed (Fig. 1a). At the upper part of the 6th lumbar vertebra near the lumbar disc, an electric drill was used to bore a hole (0.3 × 0.8 × 0.4 cm^3) from the right front to the left behind at a 30° angle to the transverse plane (Fig. 1b). After achieving hemostasis, this hole was filled with medical gelatin sponges. Then, the gelatin sponges were impregnated slowly using a syringe with 0.2 ml of a TB suspension at a concentration of 0.5 mg/ml (10^7 CFU/ml) for the infection group or 0.2 ml sterile normal saline for the control group. Finally, the incision was sutured layer by layer, and the sterile drape was fixed on the incision (Fig. 1c).

If the anesthesia depth became shallow during an operation, 2% sodium pentobarbital was administered through the indwelling tube. If massive bleeding occurred, prompt hemostasis was required and low-molecular-weight dextran was rapidly infused. Epinephrine (0.1%; 1 ml) was injected intravenously if a rabbit appeared to have slow or irregular breathing. If necessary, 5 ml of calcium chloride (1%) was intravenously administrated along with rescue measures such as chest compressions if the rabbit's life appeared to be in danger.

After surgery, the rabbits were fed alone following the principles of aseptic technique, safety, and animal ethics.

Evaluation methods: (i) General observations: Wound healing, eating, activity, and mental status of the rabbits were observed postoperatively. We excluded any rabbits with nonunion, ulceration, or infection. **(ii) Imaging examinations:** All imaging procedures were performed at 4 weeks and 8 weeks postoperatively and an X-ray examination was also performed on the day after surgery. Exposure conditions for an X-ray examination were: lateral, 45 KV, 8.0 mAs, projection distance of 110 cm; anteroposterior, 44 KV, 9.0 mAs, projection distance of 110 cm.

Examination conditions for a computed tomography (CT) examination were: 120 KV, 300 mA, FOV 250, 1-mm slice thickness, and 1-mm spacing.

Magnetic resonance (MR) images were obtained using a 1.5 T MRI system (PHILIPS, Best, Netherlands) with a multi-channel coil to scan the entire spine. All rabbits were anesthetized through an ear vein and were placed prostrate on an examination table with the hind legs first. Turbo field echo sequences with conventional T1-weighted imaging and T2-weighted imaging (T_R, 15 ms; T_E, 5.2 ms; FOV, 250 mm; slice thickness, 10 mm) were

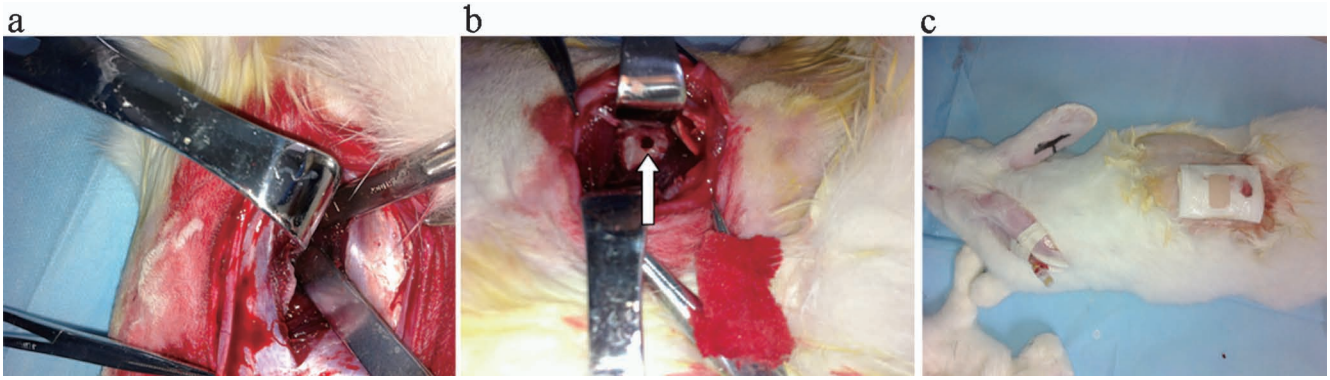

Fig. 1. (Color online) Establishment about the animal model. The muscle tissues were separated (a) and a hole (white arrow, 0.3 × 0.8 × 0.4 cm^3) was made at upper of 6th lumbar vertebrae near the lumbar disc (b). The incision was sutured layer by layer and the sterile drape was fixed on the incision (c).

applied. **(iii) Histopathological examinations:** Rabbits were sacrificed after imaging examinations were completed at 8 weeks postoperatively. We dissected out lesion tissue for histopathological examinations. Soft tissues and bone tissues were fixed by perfusion with, respectively, 10% buffered formalin and 10% buffered formaldehyde for 24–48 h before routine processing and paraffin embedding. After decalcification with 5% nitric acid, dehydration with acetone, transparentizing with xylene, and conventional embedding in embedding compound, sections (5 mm) were stained with hematoxylin and eosin (HE) and observed under a microscope. **(iv) Bacteriological tests:** Viscous pus (0.5 g) was removed from a paravertebral abscess, prepared as a mixture in 1 ml of SDS-NaOH, and then vortexed for a few seconds. After allowing to stand at room temperature for 15 min, this liquid was diluted to 50 ml with sterile phosphate buffer (0.067 M, pH = 6.8), and then centrifuged at 3,000 rpm for 15 min. The resulting precipitate was dissolved in 1 ml of sterile phosphate buffer (0.067 M, pH = 6.8), from which 0.1 ml of liquid was collected and cultured on Lowenstein-Jensen (LJ) medium at 36°C for 8 weeks. We prepared LJ medium in-house, which included $MgSO_4.7H_2O$ (0.24 g), K_2HPO_4 (2.4 g), magnesium citrate (0.6 g), sodium glutamate (7.2 g), glycerol (12 ml), distilled water (600 ml), fresh chicken eggs liquid (1,000 ml), and malachite green (20 ml). Culture results were determined on the basis of the test procedures used for bacteriological diagnosis of tuberculosis of 1995 (10).

RESULTS

General observations: Expect for 1 rabbit in the control group that suffered from a peritoneal rupture, which was repaired quickly, all other rabbits underwent surgical procedures smoothly. Adverse events in the infection group were: 1 rabbit did not eat and died the next day due to shortness of breath and listlessness; 1 rabbit ate poorly died at 9 days; 1 rabbit with nonunion, redness, and pus at the incision site at 4 weeks after surgery was excluded; 1 rabbit for which imaging examinations were completed at 8 weeks died at 4 h after inducing anesthesia; and 4 rabbits died at 7 weeks due to eating poorly and unstable vital signs. The remaining rabbits in the infection group appeared to have stable vital signs, ate well, and had stable body weights. Adverse events in the control group included 1 rabbit with nonunion, redness, and pus at the incision site at 2 weeks after surgery that was excluded and 1 that died at 11 days because of poor eating. The remaining rabbits in the control group appeared to have stable vital signs, ate well, and had stable body weights.

Imaging results: (i) X-ray examinations: On the day after surgery, X-ray examinations were performed; there were no obvious abnormalities, such as congenital malformations or bone destruction (Fig. 2a, 2b). At 4 weeks postoperatively, 3 rabbits in the infection group showed slight bone destruction on the superior borders of L5 vertebrae and slightly reduced bone densities (Fig. 2c). At 8 weeks postoperatively, 8 rabbits appeared to have bone destruction on the superior borders of L5 and L6 vertebrae, increased and uneven bone densities, rough edges of the vertebral bodies, and occasional narrowing of a disc space, 1 of which showed a scoliosis-type deformity (Fig. 2d, 2e, 2f). The rabbits in the control group exhibited no evidence of abnormal changes either at 4 weeks or at 8 weeks postoperatively. **(ii) CT examinations:** At 4 weeks postoperatively, 5 rabbits in the infection group showed slight bone destruction on the superior borders of their L5 vertebrae (Fig. 3a). At 8 weeks postoperatively, CT scan results showed evidence of bone destruction on the superior borders of L5 vertebrae in 10 rabbits (Fig. 3b). Three-dimensional reconstructions of CT scan results showed that 2 rabbits appeared to have bone destruction on the margo inferior parts of their L5 vertebrae and superior borders of L6 vertebrae and narrowing of disc spaces, 1 rabbit exhibited a scoliosis-type deformity, 4 rabbits showed psoas major asymmetric swelling, and 1 rabbit showed an obvious kyphosis deformity (Fig. 3c). Calcification or sequestrum formed in 1 rabbit and spinal canal compromise occurred in 1 rabbit (Fig. 3d). The control group of rabbits showed no evidence of abnormal changes either at 4 weeks or at 8 weeks postoperatively. **(iii) MRI examinations:** At 4 weeks postoperatively, MRI findings for 22 rabbits in the infection group showed slight bone destruction (Fig. 4a, 4b). At 8 weeks postoperatively, 15 rabbits appeared to have obvious bone destruction (Fig. 4c, 4d). Decreased sagittal T1-weighted signals (Fig. 4a) and mixed changes of sagittal T2-weighted signals (Fig. 4b) appeared in the superior borders of L5 vertebrae of these rabbits at 4 weeks postoperatively. Intervertebral disc signals between L5 and L6 vertebrae were reduced on sagittal T1-weighted (Fig. 4a) and T2-weighted images (Fig. 4b). At 8 weeks postoperatively, long T1 (Fig. 4c) and T2 (Fig. 4d) signals appeared in L5 vertebrae. Behind the L5 vertebrae, sagittal T1-weighted images had high signals (Fig. 4c) and sagittal T2-weighted images had heterogeneous high signals (Fig. 4d). The control group of rabbits showed no evidence of abnormal changes either at 4 weeks or at 8 weeks postoperatively.

The extents of tuberculosis lesions on a single vertebra were 30 ± 10.5, 61 ± 14.2, and 76 ± 11.6 as determined by X-ray, CT, and MRI examinations, respectively. CT and MRI examinations were more sensitive for detecting the tuberculosis lesions than X-ray ($P < 0.05$; Table 1). CT values in the infection group increased from 302.3 ± 20.8 HU at 4 weeks postoperatively to 469.1 ± 11.9 HU at 8 weeks postoperatively ($P < 0.05$), whereas the CT values in the control group remained essentially unchanged ($P > 0.05$; Table 2).

General anatomic observations: Fifteen rabbits with positive imaging results were sacrificed, 9 of which showed pale yellow paravertebral abscesses with diameters of 0.5 cm–5.0 cm (Fig. 5). Obvious bone destruction had occurred on the margo inferior parts of L5 vertebrae or the superior borders of L6 vertebrae. The

Table 1. The scope of the tuberculosis lesion on a single vertebral

	X-ray	CT	MRI
Scope (%)	30 ± 10.5	61 ± 14.2[1)]	76 ± 11.6[1)]
Number of vertebral	22	22	22

[1)]: compared to X-ray, $P < 0.05$.

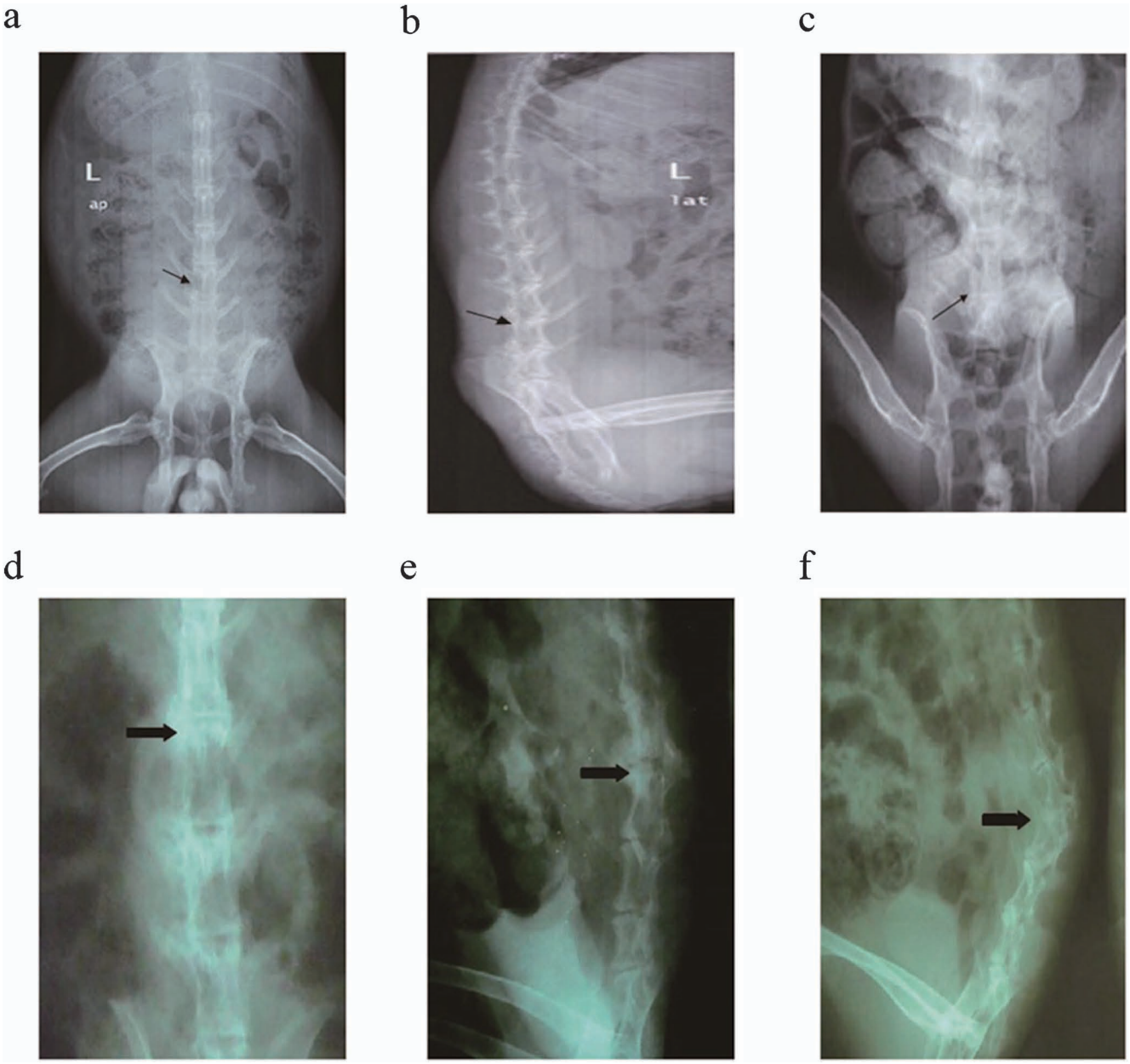

Fig. 2. (Color online) X-ray examination. The anteroposterior (a) and lateral (b) showed no obvious abnormalities in the spin of rabbits the next day after surgery. Four weeks postoperatively, the rabbit of infection group appeared slight bone destruction on the superior border of L5 vertebrae in anteroposterior (c) view. Eight weeks postoperatively, the rabbit of infection group showed bone destruction on the superior border of L5 and L6 vertebrae (d), narrowing of disc space (e), and scoliosis deformity (f).

Table 2. The CT value of the rabbits in the infection and control groups

Time after operation	CT value (HU)	
	Infection group	Control group
4 weeks	302.3 ± 20.8	252.6 ± 16.815
8 weeks	469.1 ± 11.9[1)]	267.2 ± 15.348

[1)]: compared to 4 weeks, $P < 0.05$.

livers, lungs, and spleens of these rabbits had no obvious abnormalities. No obvious paravertebral abscesses occurred in the control group rabbits or those rabbits with negative imaging results.

Histopathological detection: For the 15 rabbits with positive MRI results, histopathological examinations revealed disordered structures of trabecular bone (Fig. 6a) and inflammatory cell infiltration and necrosis of soft tissues (Fig. 6b, 6c). HE staining of vertebral sections showed infiltration by pus cells and bone structure disappearance (Fig. 6d and 6e). No abnormalities were observed in the control group (Fig. 6f).

As compared to the control group, osteoblasts in the infection group were significantly reduced (20.3 ± 5.3 vs. 50.5 ± 4.5, $P < 0.01$), whereas multinucleated osteoclasts were significantly increased (6.2 ± 2.4 vs. 2.2 ± 1.1, $P < 0.01$; Table 3).

TB culture results: Pus samples were obtained from the 15 rabbits with positive MRI findings. After culture

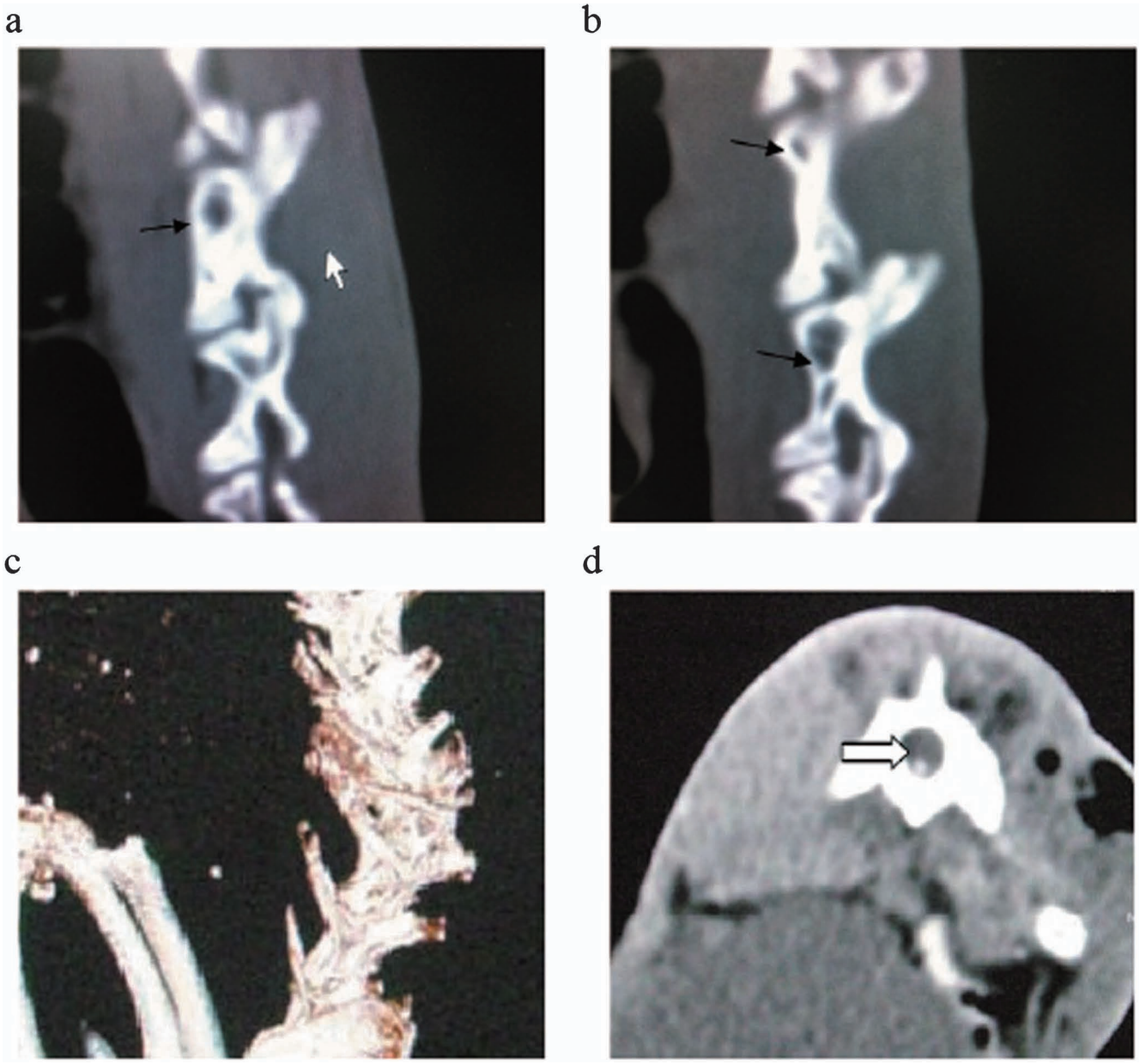

Fig. 3. (Color online) CT examination. In infection group, CT scan showed slight bone destruction on the lateral margin of L5 vertebrae (a), four weeks postoperatively. Eight weeks postoperatively, CT scan presented the evidence of bone destruction on the lateral margin of L5 vertebrae (b), and spinal canal compromise (d). Three-dimensional reconstruction CT scan showed scoliosis deformity (c).

Table 3. The number of the osteoblast and multinucleated osteoclast at the osteolysis lesions tissue in infection group and the cancellous bone tissue in control group

Cell	Infection group	Control group
Osteoblast	20.3 ± 5.3[1)]	50.5 ± 4.5
Multinucleated osteoclast	6.2 ± 2.4[1)]	2.2 ± 1.1

[1)]: compared to control group, $P < 0.01$. Total 6 sections for each sample were observed.

for 8 weeks, 10 samples had positive results with the appearance of pale yellow colonies.

DISCUSSION

Using animal models is a crucial first step in the research flow for developing new drugs and vaccines (11). There are many factors involved in the success rates of these models. In our study, the consequences of spinal infection may have depended on the animal used, the route of infection, and the bacterial dose used.

Selecting appropriate experimental animals: There are dozens of animals (12) that can be used to establish TB infection models, including mice, rats, guinea pigs, rabbits, monkeys, cattle, goats, deer, and others. As early as 1928, rabbits were used as an experimental model to study the fate of tubercle bacilli after intravenous infection (13). Subsequently, Lurie and colleagues performed extensive studies on TB using rabbits

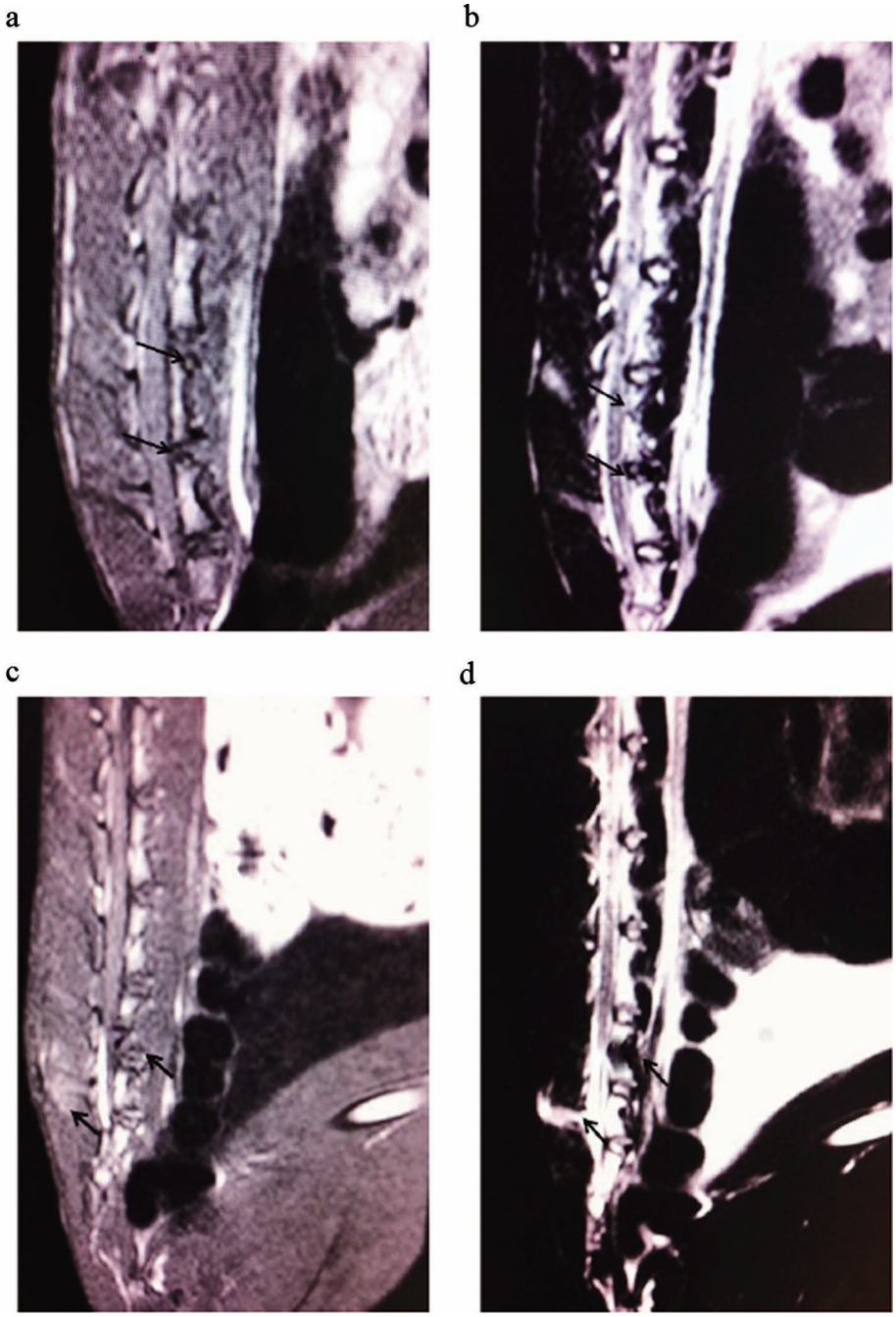

Fig. 4. (Color online) MRI examination. Four weeks postoperatively, slight bone destruction, decreased sagittal T1-weighted signal intensity (a) and mixed changes of sagittal T2-weighted signal intensity (b) were appeared in the superior border of L5 vertebrae. Intervertebral disc signal between L5 and L6 vertebrae was decreased at sagittal T1-weighted (a) and T2-weighted image (b). Eight weeks postoperatively, obvious bone destruction, long T1 (c) and T2 (d) signal were appeared in the L5 vertebrae. Behind the L5 vertebrae, sagittal T1-weighted image was high signal (c) and sagittal T2-weighted image was heterogeneous high signal (d).

as a model (14–17). Recently, rabbit models have been designed to study the efficacy of the only currently available TB vaccine, the attenuated strain of *M. bovis* bacillus Calmette-Gu'erin (BCG) (18). These considerations suggest that rabbits are useful experimental animals for studying TB infections. Additionally, rabbits are better suited for studying spinal TB because it is simple to perform basic surgical procedures on their spines. Because rabbits have good physiques and have some immunity for *M. tuberculosis*, they can be infected by bacteria under the control of weight and exercise.

Infection route: In general, spinal TB infection can be achieved through local direct inoculation, indirect paravertebral inoculation, and vasa vasorum injection. The advantages of local direct inoculation are clear lesion locations and the short time for infection to progress. In contrast, indirect paravertebral inoculation may result in the spread of *M. tuberculosis* into local soft tissues, which results in dispersed development and ambiguous lesions. Although the route of vasa vasorum injection is the most similar to the natural route of *M. tuberculosis* infection, experiments and operations are

difficult because the terminal arteritis that nourish vertebral bodies are relatively small, where *M. tuberculosis* can readily form emboli. Inspired by a study (19) that established an animal model of pulmonary tuberculosis by direct inoculation following bronchoscopy, we implanted *M. tuberculosis* bacteria directly into vertebral bodies to establish a spinal TB model.

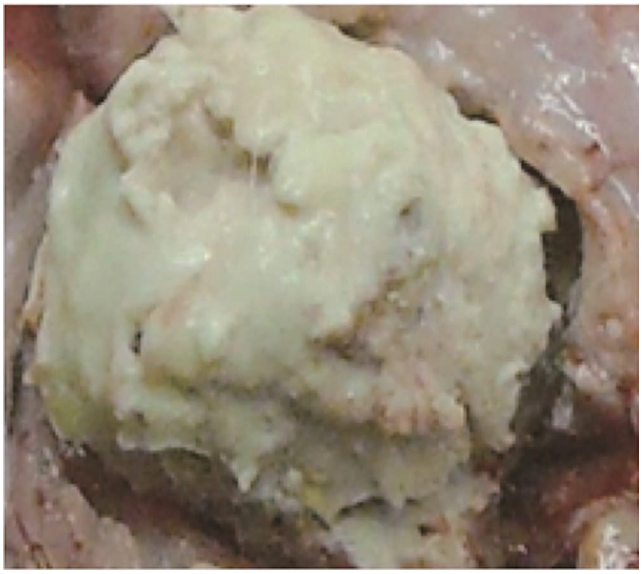

Fig. 5. (Color online) Anatomic observation of pale yellow paravertebral abscess.

Surgical approach: The vertebral bodies of New Zealand white rabbits are very thin. Thus, we chose the 6th lumbar vertebra, which is relatively larger, to perform surgery. The subcutaneous fascia and muscles should be separated carefully to avoid injury to vessels and nerves. The tissues around the 6th lumbar vertebrae and 5–6th intervertebral discs should be stripped away thoroughly to avoid infections in soft tissues. In addition, this vertebra is near the ilium and positioning is easy.

This vertebral body is loose and can easily be penetrated and result in injury to the spinal cord when drilling. Thus, the intensity of drilling should not be too great and the hole should not be too deep. A peritoneal lateral surgical approach is usually used to expose the vertebral body. However, the rabbit's peritoneum is very thin and a complete retroperitoneal strip is difficult. Wang (20) proposed that a lateral approach was a better way with a short operating time and with limited postoperative complications. In preliminary experiments, we used a posterior approach and a lateral approach. With the posterior approach, the mean operation time for exposure was short at only 7 min, although the best vertebral plane was not shown very well. Thus, spinal canal penetration was quite frequent and resulted in 1 death and 2 rabbits with hind limb paralysis. By comparison, the mean operation time for exposure, when using a lateral approach, was longer at 12 min; although, the vertebral body and intervertebral disc were adequately exposed for performing an operation under direct vision. In addition, blood loss was less

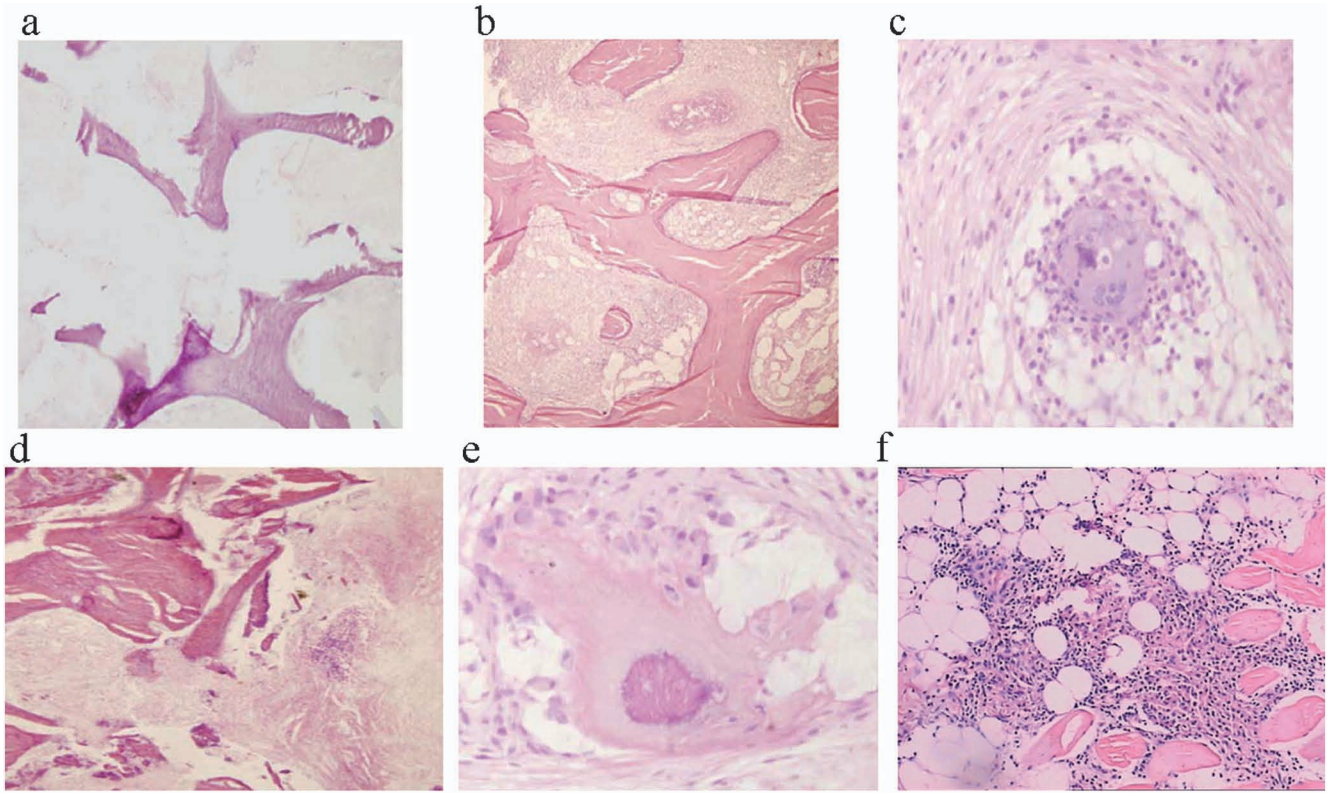

Fig. 6. (Color online) HE stain. Disordered structure of trabecular bone structure (a, 100 ×). The infiltration of inflammatory cells and the necrosis in the soft tissue (b, 100 × and c, 400 ×). The infiltration of pus cells and disappearing of bone structure in the vertebral (d, 100 × and e, 400 ×). No abnormality was observed in the control group (f, 40 ×).

than with the posterior approach and all rabbits survived.

Thus, in this study, we opted for the lateral approach to expose the vertebral bodies and intervertebral discs. Choosing the best surgical approach for exposure can reduce the incidence of surgical accidents and complications and thus improve the success rate for establishing a model. Moreover, the gelatin sponges impregnated with a TB suspension for infection reduced the diffusion of the bacterial suspension and increased the contact time between bone tissues and the bacterial suspension.

Infection dose: The H37Rv strain, which has retained the virulence of *M. tuberculosis*, is a widely used laboratory strain (21). A bacterial suspension should be prepared on the day of surgery and should be used within 12 h at a low temperature to ensure bacterial activity. The dose of H37Rv used is critical for the success rate during model establishment, as a very high dose will cause widespread lesions and even death, while a very low dose may result in a low positive rate for local lesions. In preliminary experiments, when 5 mg/ml of a TB suspension (0.3 ml) was used, all New Zealand white rabbits died after infection and 5 mg/ml of TB suspension (0.2 ml) resulted in death of half of the rabbits. Fortunately, the survival rate was as high as 93% when we used 0.5 mg/ml (0.2 ml, 1×10^7 CFU) of a TB suspension to infect rabbits.

Imaging findings: An early diagnosis of spinal TB is often difficult due to the lack of specific clinical manifestations during the early stage. Recent improvements in diagnostic tools and techniques, such as imaging techniques and the polymerase chain reaction, have made an earlier diagnosis possible (22). Achieving an accurate diagnosis of early spinal TB through imaging techniques is important for treatment. The X-ray, CT, and MRI characteristics of spinal TB have been well documented.

X-ray diagnosis of spinal TB is the most basic and most commonly used method (23). Plain X-ray characteristics of spinal TB include osseous destruction in vertebral bodies, narrowing of intervertebral disc spaces, and gibbous deformities of the spine (24). Conforming to these, we detected the typical X-ray characteristics in infected rabbits in that 2 rabbits showed mild osseous destruction at 4 weeks postoperatively and 6 rabbits showed osseous destruction or narrowing of intervertebral disc spaces at 8 weeks postoperatively. However, X-ray findings generally occur late, which often result in a missed diagnosis and delayed treatment.

CT imaging is superior to plain radiography for demonstrating the presence of paraspinal abscesses (25). Calcifications in paraspinal collections are best observed on CT scanning, which is also better for demonstrating the numerous small bone fragments that may remain in the area of destroyed bone. In addition, CT scanning can clearly demonstrate bony sclerosis in addition to destruction within vertebral bodies (23). Paravertebral abscesses that involve the psoas can also be identified by CT, although epidural abscesses are better defined by MRI (26). In the present study, typical characteristics, including calcification, sequestrum, narrowing of disc spaces, scoliosis-type deformity, and psoas major asymmetric swelling, were all evidenced by CT imaging in our infection group.

MRI imaging provides for excellent definition of paravertebral soft tissue swelling or paravertebral abscess, vertebral body destruction, and other changes (27, 28). Characteristic changes are usually homogeneously reduced T1-weighted signal intensity and heterogeneously increased T2-weighted signal intensity (29). In our study, similar MRI findings were found in our experimental rabbit model. At 4 weeks postoperatively, 7 rabbits in the infection group showed obvious bone destruction with reduced T1-weighted signal intensity and heterogeneously increased T2-weighted signal intensity. At 8 weeks postoperatively, 15 rabbits appeared to have obvious bone destruction after MRI examinations, which was greater than that detected by X-rays and CT imaging. Thus, compared with X-rays and CT imaging, MRI is more sensitive for diagnosing spinal TB.

Histopathological detection: The major finding of spinal TB is caseous necrosis followed by a proliferative lesion, which is confirmed by HE staining. In this study, histopathological examinations revealed inflammatory cell infiltration into soft tissues as well as necrosis in 15 rabbits with positive MRI results. In addition, the trabecular bone structure was disorderd and fractured in the diseased vertebral bodies.

TB culture: Imaging examinations are excellent for detecting spinal TB. However, microbiological diagnosis is essential. *M. tuberculosis* strain H37Rv is a slow-growing pathogen that requires a relatively long culture period (30). It can grow in LJ medium, 7H9 broth medium, blood agar medium, and others (31–33). In this study, rabbit pus specimens were cultured using modified LJ medium for 4 weeks and the positive rate was 67%. Piersimoni et al. reported that the sensitivity of LJ medium was less than that of a MB/BacT ALERT 3D System (34). Thus, if available, the MB/BacT ALERT 3D System would be a better choice.

In conclusion, by inoculating local vertebral bodies of New Zealand white rabbits with an appropriate dose of strain H37Rv, we established a model of spinal TB, the pathological changes of which were similar to those in human spinal TB. This method was simple and with a relatively high success rate, which may provide some contributions to studies on the pathology of spinal TB and for new drug or vaccine screening.

One limitation of our study was that CT or MRI enhanced scans and special sequence MRI scanning were not performed; thus, we could not determine lesion progression. Another limitation was the high mortality rate. Additional research will be needed to resolve these issues.

Acknowledgments This study was supported by the National Natural Science Foundation of China (NO. 81160173). We wish to express our warm thanks to Fenghe (Shanghai) Information Technology Co., Ltd. Their ideas and help gave a valuable added dimension to our research.

Conflict of interest None to declare.

REFERENCES

1. Garg RK, Somvanshi DS. Spinal tuberculosis: a review. J Spinal Cord Med. 2011;34:440-54.
2. Gautam MP, Karki P, Rijal S, et al. Pott's spine and paraplegia. JNMA J Nepal Assoc. 2005;44;106-15.
3. Trecarichi EM, Di Meco E, Mazzotta V, et al. Tuberculous spondylodiscitis: epidemiology, clinical features, treatment, and out-

come. Eur Rev Med Pharmacol Sci. 2012;16:58-72.
4. Delogu G, Zumbo A, Fadda G. Microbiological and immunological diagnosis of tuberculous spondylodiscitis. Eur Rev Med Pharmacol Sci. 2012;Suppl 2:73-8.
5. Gupta UD, Katoch VM. Animal models of tuberculosis. Tuberculosis. 2005;85:277-93.
6. Mora FB, Llamedo LP. Experimental studies on the treatment of bone and joint tuberculosis with dihydrostreptomycin and isonicotinic acid hydrazide. J Bone Joint Surg Am. 1955;37-A(1): 156-68.
7. Ioerger TR, Feng Y, Ganesula K, et al. Variation among genome sequences of H37Rv strains of Mycobacterium tuberculosis from multiple laboratories. J Bacteriol. 2010;192:3645-53.
8. Fremond CM, Togbe D, Doz E, et al. IL-1 receptor-mediated signal is an essential component of MyD88-dependent innate response to Mycobacterium tuberculosis infection. J Immunol. 2007;179:1178-89.
9. Wilkinson KA, Kon OM, Newton SM, et al. Effect of treatment of latent tuberculosis infection on the T cell response to Mycobacterium tuberculosis antigens. J Infect Dis. 2006;193:354-9.
10. Zhuang Y, Wang G, Di B. Test procedures for bacteriological diagnosis of tuberculosis Chinese Anti-Tuberculosis Assoc. 1996; 18:28-31.
11. Druilhe P, Hagan P, Rook GA. The importance of models of infection in the study of disease resistance. Trends Microbiol. 2002;10 (10 Suppl):S38-46.
12. Dietrich G, Viret J-F, Hess J. Mycobacterium bovis BCG-based vaccines against tuberculosis: novel developments. Vaccine. 2003;21:667-70.
13. Lurie MB. The fate of human and bovine tubercle bacilli in various organs of the rabbit. J Exp Med. 1928;48:155-82.
14. Lurie MB. The correlation between the histological changes and the fate of living tubercle bacilli in the organs of tuberculous rabbits. J Exp Med. 1932;55:31-54.
15. Lurie MB. Nature of inherited natural resistance to tuberculosis. in Proceedings of the Society for Experimental Biology and Medicine. Society for Experimental Biology and Medicine (New York, NY). 1938;39:181-7. Royal Society of Medicine.
16. Lurie MB, Zappasodi P. Heredity, Constitution and Tuberculosis, an Experimental Study. Baltimore, ML: National Tuberculosis Association; 1941. p.1-125.
17. Lurie MB, Dannenberg AM. Macrophage function in infectious disease with inbred rabbits. Bacteriol Rev. 1965;29:466-76.
18. Tsenova L, Harbacheuski R, Sung N, et al. BCG vaccination confers poor protection against M. tuberculosis HN878-induced central nervous system disease. Vaccine. 2007;25:5126-32.
19. Capuano SV 3rd, Croix DA, Pawar S, et al. Experimental Mycobacterium tuberculosis infection of cynomolgus macaques closely resembles the various manifestations of human M. tuberculosis infection. Infect Immun. 2003;71:5831-44.
20. Wang F, Qu D, Jin D. Method of lateral appro Infect Immun ach for exposure the lumbar disc and injection within the lumbar disc in rabbit. Chinese J Exp Surg 2003;20:204.
21. Cole ST. Comparative and functional genomics of the Mycobacterium tuberculosis complex. Microbiology. 2002;148:2919-28.
22. Lee SH, Sung JK, Park YM. Single-stage transpedicular decompression and posterior instrumentation in treatment of thoracic and thoracolumbar spinal tuberculosis: a retrospective case series. J Spinal Disord Tech. 2006;19:595-602.
23. Teo EL, Peh WC. Imaging of tuberculosis of the spine. Singapore Med J. 2004;45:439-44.
24. Shanley DJ. Tuberculosis of the spine: imaging features. AJR Am J Roentgenol. 1995;164:659-64.
25. Joseffer SS, Cooper PR. Modern imaging of spinal tuberculosis. J Neurosurg Spine. 2005;2:145-50.
26. Cottle L, Riordan T. Infectious spondylodiscitis. J Infection. 2008;56:401-12.
27. Tyrrell PN, Cassar-Pullicino VN, McCall IW. Spinal infection. Eur Radiol. 1999;9:1066-77.
28. Moore SL, Rafii M. Imaging of musculoskeletal and spinal tuberculosis. Radiol Clin North Am. 2001;39:329-42.
29. Sinan T, AI-Khawari H, Ismail M, et al. Spinal tuberculosis: CT and MRI features. Ann Saudi Med. 2004;24:437-41.
30. Cole ST, Brosch R, Parkhill J, et al. Deciphering the biology of Mycobacterium tuberculosis from the complete genome sequence. Nature. 1998;393:537-44.
31. Dieli F, Troye-Blomberg M, Ivanyi J, et al. Granulysin-dependent killing of intracellular and extracellular Mycobacterium tuberculosis by Vγ9/Vδ2 T lymphocytes. J Infect Dis. 2001;184:1082-5.
32. Coban AY, Cihan CC, Bilgin K, et al. Blood agar for susceptibility testing of Mycobacterium tuberculosis against first-line drugs. Int J Tuberc Lung Dis. 2006;10:450-3.
33. Sethi S, Sharma S, Sharma SK, et al. Drug susceptibility of Mycobacterium tuberculosis to primary antitubercular drugs by nitrate reductase assay. Indian J Med Res. 2004;120:468-71.
34. Piersimoni C, Scarparo C, Callegaro A, et al. Comparison of MB/BacT ALERT 3D system with radiometric BACTEC system and Lowenstein-Jensen medium for recovery and identification of mycobacteria from clinical specimens: a multicenter study. J Clin Microbiol. 2001;39:651-7.